

1-1-2014

## Occupied and unoccupied electronic structure of Na doped MoS<sub>2</sub>(0001)

Takashi Komesu

Duy Le

*University of Central Florida*

Xin Zhang

Quan Ma

Eike F. Schwier

*See next page for additional authors*

Find similar works at: <https://stars.library.ucf.edu/facultybib2010>

University of Central Florida Libraries <http://library.ucf.edu>

This Article is brought to you for free and open access by the Faculty Bibliography at STARS. It has been accepted for inclusion in Faculty Bibliography 2010s by an authorized administrator of STARS. For more information, please contact [STARS@ucf.edu](mailto:STARS@ucf.edu).

---

### Recommended Citation

Komesu, Takashi; Le, Duy; Zhang, Xin; Ma, Quan; Schwier, Eike F.; Kojima, Yohei; Zheng, Mingtian; Iwasawa, Hideaki; Shimada, Kenya; Tangiguchi, Masaki; Bartels, Ludwig; Rahman, Talat S.; and Dowben, P. A., "Occupied and unoccupied electronic structure of Na doped MoS<sub>2</sub>(0001)" (2014). *Faculty Bibliography 2010s*. 5588.

<https://stars.library.ucf.edu/facultybib2010/5588>



---

**Authors**

Takashi Komesu, Duy Le, Xin Zhang, Quan Ma, Eike F. Schwier, Yohei Kojima, Mingtian Zheng, Hideaki Iwasawa, Kenya Shimada, Masaki Tangiguchi, Ludwig Bartels, Talat S. Rahman, and P. A. Dowben

# Occupied and unoccupied electronic structure of Na doped MoS<sub>2</sub>(0001)

Cite as: Appl. Phys. Lett. **105**, 241602 (2014); <https://doi.org/10.1063/1.4903824>

Submitted: 23 October 2014 . Accepted: 27 November 2014 . Published Online: 15 December 2014

Takashi Komesu, Duy Le , Xin Zhang, Quan Ma, Eike F. Schwier, Yohei Kojima, Mingtian Zheng, Hideaki Iwasawa, Kenya Shimada, Masaki Taniguchi, Ludwig Bartels, Talat S. Rahman, and P. A. Dowben 



View Online



Export Citation



CrossMark

## ARTICLES YOU MAY BE INTERESTED IN

[p-type doping of MoS<sub>2</sub> thin films using Nb](#)

Applied Physics Letters **104**, 092104 (2014); <https://doi.org/10.1063/1.4867197>

[Band structure characterization of WS<sub>2</sub> grown by chemical vapor deposition](#)

Applied Physics Letters **108**, 252103 (2016); <https://doi.org/10.1063/1.4954278>

[Electronic structure of monolayer 1T'-MoTe<sub>2</sub> grown by molecular beam epitaxy](#)

APL Materials **6**, 026601 (2018); <https://doi.org/10.1063/1.5004700>

Applied Physics Reviews  
Now accepting original research

2017 Journal  
Impact Factor:  
**12.894**

AIP  
Publishing

## Occupied and unoccupied electronic structure of Na doped MoS<sub>2</sub>(0001)

Takashi Komesu,<sup>1</sup> Duy Le,<sup>2</sup> Xin Zhang,<sup>1</sup> Quan Ma,<sup>3</sup> Eike F. Schwier,<sup>4</sup> Yohei Kojima,<sup>5</sup> Mingtian Zheng,<sup>5</sup> Hideaki Iwasawa,<sup>4</sup> Kenya Shimada,<sup>4</sup> Masaki Taniguchi,<sup>4,5</sup> Ludwig Bartels,<sup>3</sup> Talat S. Rahman,<sup>2</sup> and P. A. Dowben<sup>1</sup>

<sup>1</sup>Department of Physics and Astronomy, Theodore Jorgensen Hall, 855 N 16th St., University of Nebraska, Lincoln, Nebraska 68588-0299, USA

<sup>2</sup>Department of Physics, University of Central Florida, 4000 Central Florida Blvd., Orlando, Florida 32816, USA

<sup>3</sup>Department of Chemistry and the Materials Science and Engineering Program, University of California - Riverside, Riverside, California 92521, USA

<sup>4</sup>Hiroshima Synchrotron Radiation Center, Hiroshima University, Higashi-Hiroshima 739-0046, Japan

<sup>5</sup>Graduate School of Science, Hiroshima University, Higashi-Hiroshima 739-8526, Japan

(Received 23 October 2014; accepted 27 November 2014; published online 15 December 2014)

The influence of sodium on the band structure of MoS<sub>2</sub>(0001) and the comparison of the experimental band dispersion with density functional theory show excellent agreement for the occupied states (angle-resolved photoemission) and qualitative agreement for the unoccupied states (inverse photoemission spectroscopy). Na-adsorption leads to charge transfer to the MoS<sub>2</sub> surface causing an effect similar to n-type doping of a semiconductor. The MoS<sub>2</sub> occupied valence band structure shifts rigidly to greater binding with little change in the occupied state dispersion. Likewise, the unoccupied states shift downward, approaching the Fermi level, yet the amount of the shift for the unoccupied states is greater than that of the occupied states, effectively causing a narrowing of the MoS<sub>2</sub> bandgap. © 2014 AIP Publishing LLC.

[<http://dx.doi.org/10.1063/1.4903824>]

Alkali metal adsorption on MoS<sub>2</sub>(0001) and the related metal dichalcogenides MX<sub>2</sub> (with M = Mo, W, and X = S, Se) is an effective way to characterize the changes to band structure that occur upon charge transfer and/or n-type doping. In the context of nanoscale electronics, charge transfer to MoX<sub>2</sub> layers by means of electrostatic gating has been employed to change their transport properties,<sup>1-5</sup> rendering a good understanding of the effect of extrinsic charge doping an important step towards functional MX<sub>2</sub>-based electronic and spintronic devices. Indeed, alkali metal potassium doping has been used to make an n-doped field effect transistor to construct an inverter based on WSe<sub>2</sub>.<sup>5</sup> The MX<sub>2</sub>-Na interaction is, however, not only relevant for electronic applications but also in several different areas: for instance, sodium-ion batteries (SIBs) have been discussed<sup>6,7</sup> as an alternative to lithium ion batteries and 2-D layered nanomaterials, such as the MX<sub>2</sub>, may be capable of accommodating the large volumetric strains during charging and discharging, while remaining high-capacity sodium host materials. In addition, alkali metal adsorption has significant influence on the catalytic properties of MoS<sub>2</sub>.<sup>8-10</sup>

Although there are many efforts to experimentally characterize the band structure of MoS<sub>2</sub>,<sup>11-16</sup> as well as of monolayer MoS<sub>2</sub>,<sup>14,17</sup> the aspect of intrinsic and extrinsic doping has not been addressed by methods that allow access to both occupied and unoccupied band structure/alignment.<sup>16</sup> Worse yet is our understanding of the influence of alkali metals on the electronic structure of MoS<sub>2</sub>.<sup>8-10,17-21</sup> This study addresses some of the deficiencies in our understanding in charge donor modifications to the MoS<sub>2</sub>(0001) band structure through a combined investigation of both the unoccupied and occupied electronic structure, detailing the changes in electronic structure that accompany Na adsorption, but without the complexities associated with intercalation.<sup>17</sup>

The occupied states were measured by high-resolution angle-resolved photoemission spectroscopy (ARPES), performed at the linear undulator beamline (BL-1)<sup>22</sup> at the Hiroshima Synchrotron Radiation Center (HiSOR) at Hiroshima University, Japan, described elsewhere.<sup>16</sup> The energy resolution was limited by temperature, not the instrument, and estimated to be ~30 meV for ARPES performed at room temperature. The angular resolution was 0.7°, corresponding to a wave vector resolution of  $0.035 \pm 0.005 \text{ \AA}^{-1}$  for  $h\nu = 34 \text{ eV}$  at the Fermi level ( $E_F$ ).

The unoccupied state spectra were acquired in separate ultrahigh vacuum systems equipped with the inverse photoemission (IPES), low energy electron diffraction (LEED), and x-ray photoemission spectroscopy (XPS). The inverse photoemission experiments were acquired in the isochromat mode with a commercial high resolution electron gun (Kimball Physics) combined with channeltron-based photon detector (Omnivac), as well as using an electron gun based on the photoemission from cesiated GaAs, with a Geiger Muller photodetector, the latter as described elsewhere.<sup>23</sup> The results shown here are from the inverse photoemission spectra obtained with the channeltron-based photon detector. The IPES systems were capable of angle resolved measurements to extract wave vector dependence of the unoccupied states. The total IPES resolution was about 400 meV. Spectra were taken along two different crystallographic directions with various electron incidence angles, corresponding to the  $\bar{\Gamma}$  to  $\bar{K}$  direction to  $\sim 1.0 \text{ \AA}^{-1}$  and to the  $\bar{\Gamma}$  to  $\bar{M}$  direction to  $\sim 0.7 \text{ \AA}^{-1}$ , in steps of 5°. Throughout the discussion, the binding energies are referenced to the Fermi level ( $E - E_F$ ) of an Au film electrically connected to the sample.

Samples were cleaved *in-situ* for both the photoemission and inverse photoemission measurements, and surface order

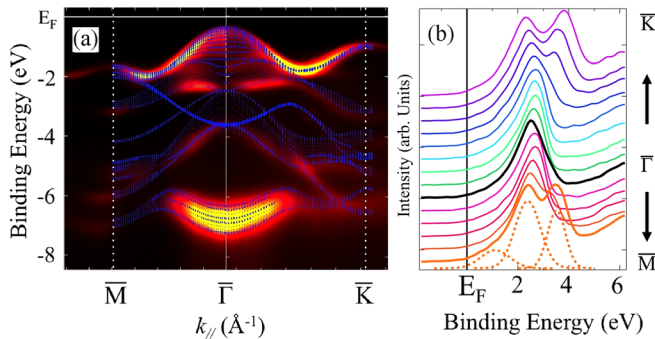


FIG. 1. (a) The density functional theory surface and near surface weighted bands (blue dots) of MoS<sub>2</sub>(0001) are compared to the display of the experimental band structure (red and yellow, with yellow indicating greater intensities) obtained from ARPES, for the p-polarization geometry and 34 eV photon energy along the combined  $\bar{M}$ - $\bar{\Gamma}$ - $\bar{K}$  symmetry directions of the surface Brillouin zone. Binding energies are denoted as  $E-E_F$ . (b) The experimental set of angle-resolved IPES spectra, with a thick black spectrum referring to  $\bar{\Gamma}$  (normal incident IPES results), along both  $\bar{M}$ - $\bar{\Gamma}$ - $\bar{K}$  symmetry directions.

and orientation were confirmed by LEED, as described in Ref. 16. Sodium dosing onto MoS<sub>2</sub>(0001) was achieved by means of a standard Na getter (SAES). The vacuum remained better than  $10^{-10}$  Torr throughout the experiments and the Na/MoS<sub>2</sub>(0001) surface was routinely characterized by X-ray core level photoemission (XPS) to verify the absence of surface contamination. All measurements were carried out at room temperature to ensure adsorption of no more than one monolayer of Na, and to suppress the time-dependent intercalation as has been described for K on MoS<sub>2</sub> at low temperatures.<sup>17</sup>

As noted elsewhere, the experimental band structure (red and yellow in Figure 1(a)) is seen to be in excellent agreement with surface weighted band structure obtained from density functional theory (DFT) calculations using the super cell method with a plane-wave basis set (at a cutoff energy of 500 eV) and the projector-augmented wave (PAW)<sup>24,25</sup> technique as implemented in the Vienna *ab-initio* Simulation Package (VASP),<sup>26,27</sup> as detailed in Ref. 16. The van der Waals interactions are treated using the DFT-D3 approximation.<sup>28</sup> This agreement between theory and experiment for the occupied valence states of clean MoS<sub>2</sub>(0001) surface is seen along the  $\bar{\Gamma}$ - $\bar{K}$  and  $\bar{\Gamma}$ - $\bar{M}$  directions of the surface Brillouin zone.

Figure 1(b) shows a selection of IPES spectra along the high symmetry directions of MoS<sub>2</sub>(0001) surface Brillouin zone. IPES is a very low intensity measurement, so the experimental band structure measurements include far less wave vector sampling than angle-resolved photoemission measurements of Figure 1(a). Nonetheless, there is clear evidence of dispersion for multiple bands along both symmetry lines,  $\bar{\Gamma}$ - $\bar{M}$ - $\bar{K}$ . The experimental wave vector dependent band mapping for the unoccupied states shows the trends expected from theory (DFT), but the agreement is not nearly as good as seen for the occupied states, as summarized in Figure 2. The experimental band structure of the unoccupied states, while in reasonable agreement with the expectations of DFT close to  $E_F$  (green), diverges significantly from the DFT predictions well above the Fermi level (red and blue). It is a known problem that DFT must be rescaled for

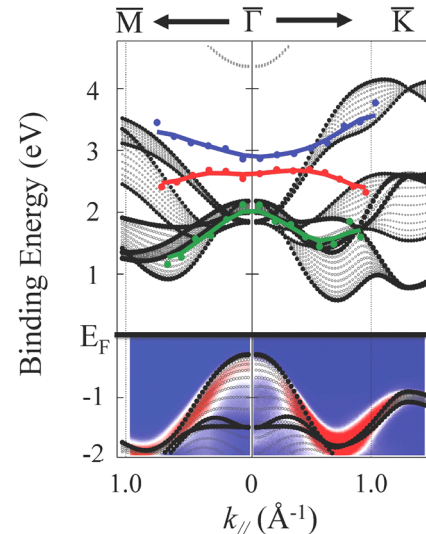


FIG. 2. The combined occupied and unoccupied band dispersion obtained from photoemission and inverse photoemission (Figure 1) along both  $\bar{M}$ - $\bar{\Gamma}$ - $\bar{K}$  symmetry directions. Those black dots are the results of the density functional theory for the surface and near surface weighted bands of MoS<sub>2</sub>(0001) calculation and overlapped on the experimental results, in the region of the Fermi level both below (ARPES) and above (IPES)  $E_F$ , respectively.

comparison with experimental results for unoccupied states.<sup>29,30</sup> Here, the electronic band structure along the  $\bar{\Gamma}$ - $\bar{K}$ - $\bar{M}$ - $\bar{\Gamma}$  directions were calculated with 159 k-points, but no corrections were made for finite temperature or final state effects in our model calculations.

From the combined photoemission and inverse photoemission measurements, we find an indirect band gap of  $1.4 \pm 0.2$  eV, close to the expected MoS<sub>2</sub> 1.29 eV indirect band gap,<sup>31</sup> but much larger than the calculated band gap of density functional theory of 0.90 eV, as is generally expected. The placement of the Fermi level closer to the valence band maximum, than the conduction band minimum cannot be taken as an indication of a more p-type material, while there is no evidence of charging in our measurements, band bending in the region of the surface cannot, *a priori*, be excluded.

The deposition of Na on MoS<sub>2</sub>(0001) leads to an increase in the valence band binding energies by  $\sim 0.5$  eV, as illustrated in Figure 3. Figures 3(a)–3(d) show the experimental occupied band structure of clean MoS<sub>2</sub>(0001) along both the  $\bar{\Gamma}$ - $\bar{K}$  symmetry direction (Figures 3(a) and 3(b)) and the  $\bar{\Gamma}$ - $\bar{M}$  symmetry direction (Figures 3(c) and 3(d)) before (Figures 3(a) and 3(c)) and after (Figures 3(b) and 3(d)) Na exposure. We observe a rigid shift of the occupied valence bands to greater binding energies practically independent of symmetry direction and wave vector. This binding energy increase (shift) is greater than the roughly 100 to 150 meV shift reported for Na on WSe<sub>2</sub>,<sup>32</sup> but less than the approximately 0.5 to 0.84 eV, 0.6 eV, and 0.75 eV shifts seen for Cs, Li, K, respectively, on MoS<sub>2</sub>.<sup>21</sup> As with Na adsorption on WSe<sub>2</sub> at room temperature,<sup>32</sup> we find evidence for only a single 1s Na core level and multiple 2p shallow core level that might be an indication of multiple site locations but not intercalation (see the supplementary material<sup>33</sup>).

We attribute the binding energy shifts largely to initial state effects resulting from charge doping of the MoS<sub>2</sub> surface leading to band bending or possibly similar to alkali



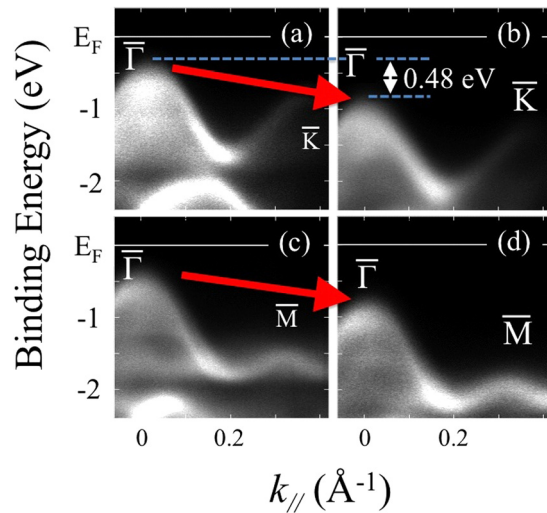


FIG. 3. The experimental band mapping of MoS<sub>2</sub>(0001) along the high symmetry lines: (c) and (d) for along the  $\bar{\Gamma}$ -M, and (a) and (b) for along the  $\bar{\Gamma}$ -K symmetry directions. The panels (a) and (c) are for clean MoS<sub>2</sub>(0001), while (b) and (d) following Na exposure to MoS<sub>2</sub> (saturation at room temperature). The total shift seen in the photoemission is about 0.5 eV, largely independent of wave vector.

metal doping of organic thin films.<sup>34,35</sup> This is also consistent with theory, as seen in Figure 4(c), where with only a  $1/4$  monolayer of Na on MoS<sub>2</sub>(0001), the six layer DFT slab calculation shows the system metallic with an appreciable Na weighted density of states at  $\bar{K}$  and  $\bar{M}$  just below the conduction band minimum of MoS<sub>2</sub>(0001), which now crosses the Fermi level. The photoemission spectra show a weak states near the Fermi level in the vicinity of  $\bar{K}$  and  $\bar{M}$ , induced by Na adsorption, and not seen for clean MoS<sub>2</sub>(0001). These new states, that accompany alkali metal adsorption on MoS<sub>2</sub>(0001), are expected from the calculated band structures for greater than  $1/4$  monolayer of Na on MoS<sub>2</sub>(0001)

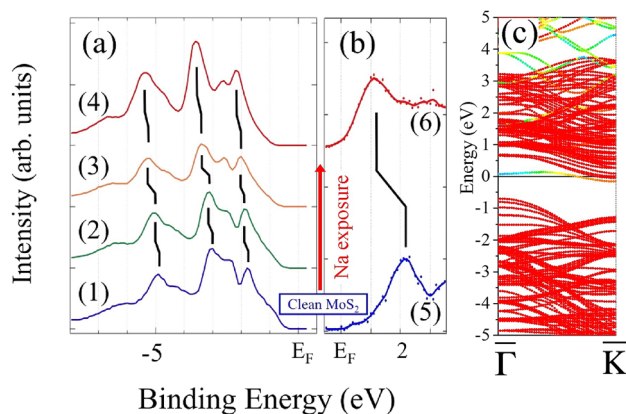


FIG. 4. The experimental spectra for both (a) photoemission (occupied) at normal emission and (b) inverse photoemission (unoccupied) at normal incidence or about the  $\bar{\Gamma}$  for both occupied and unoccupied states. The photoemission (a1) and inverse photoemission (b5) spectra for clean MoS<sub>2</sub> are compared the photoemission spectra (a2), (a3), (a4), and inverse photoemission spectrum (b6) for increasing Na coverages on MoS<sub>2</sub>(0001), with spectra (a4) and (b6) taken for saturation at room temperature. This illustrates changes in electronic structure with increasing Na coverages on MoS<sub>2</sub>. The total shifts on photoemission and inverse photoemission are roughly 0.5 eV and 1.0 eV, respectively. (c) shows the calculated six layer slab band structure (DFT) for  $1/4$  ( $2 \times 2$ ) Na adlayer on MoS<sub>2</sub>(0001), with a strongly Na weighted occupied density of states below the MoS<sub>2</sub> conduction band.

and reported previously.<sup>17,21</sup> Intercalation of K, below surface layer of single crystal MoS<sub>2</sub>, has been seen to result in a band structure with greater binding energies,<sup>26</sup> as seen here, but the dispersion of the states at the top of the valence band structure changes dramatically, resulting in a band structure somewhat more characteristic of an MoS<sub>2</sub>(0001) monolayer. This alteration in the placement of the valence band maximum,<sup>26</sup> with alkali metal adsorption, is not seen here, as is evident in Figures 3(a)–3(d).

Figure 4 juxtaposes the shift of the occupied states with increasing sodium adsorption to the shift found for the unoccupied states between the bare and the Na room temperature saturated surface of MoS<sub>2</sub>(0001). This complementary set of photoemission and inverse photoemission spectra shows that the energy shift that occurs with Na exposure to MoS<sub>2</sub>(0001) is 0.5 eV for photoemission and 1.0 eV for inverse photoemission, respectively, resulting in a net lowering of the apparent bandgap by  $\sim 0.5$  eV corresponding to more than  $1/3$  of its native value. This difference in the binding energy shifts observed for occupied (valence) and unoccupied (conduction) electronic structure, that accompanies Na exposure to MoS<sub>2</sub>(0001), is a strong indication that the band structure is perturbed either in the initial state, leading to a closure of the band gap, or in the final state, due to a change in metallicity. Initial state effects, which leave the band structure otherwise unaffected, as in the case of simple extrinsic charge doping, should affect both occupied and unoccupied states equally and in the same direction. In contrast, differences in the shifts seen for the unoccupied states (inverse photoemission) and occupied states (photoemission) are indicative of either final state effects or changes to the initial state band structure that lead to a closure of the band gap. Prior work attributed differences in the shifts seen for the unoccupied (inverse photoemission) and occupied states (photoemission) to final state effects<sup>36,37</sup> and frequently final state effects are most evident in the unoccupied state band structure. For molecular thin film systems, increased screening in the final state, affects more profoundly the inverse photoemission than the direct photoemission, leading to an apparent reduction in the highest occupied molecular orbital (HOMO) to the lowest unoccupied molecular orbital (LUMO) gap.<sup>36</sup> This is consistent with the increased metallic character evident in our DFT calculations for Na coverages of  $1/4$  monolayer and above, with a monolayer of Na making MoS<sub>2</sub>(0001) fully metallic, leaving no bandgap whatsoever in the six layer slab calculation. Alternatively, Na adsorption is seen to affect the band structure of MoS<sub>2</sub>(0001), and most significantly the unoccupied bands (Figure 4(c)), with a decrease in the gap of the MoS<sub>2</sub>(0001) weighted density of states between 13% and 43%, corresponding to the variation of Na coverage from  $1/16$  monolayer to  $1/4$  monolayer Na. A full monolayer of Na on a six layer slab of MoS<sub>2</sub> is found to be fully metallic, with no gap in the region of the chemical potential (the Fermi level), but the decrease in the gap of the heavily weighted MoS<sub>2</sub>(0001) density of states of only about 12%. Band bending, as suggested for Rb on WSe<sub>2</sub>,<sup>38</sup> would also have a more profound effect on the unoccupied states, than the occupied states.

The fact that the band gap decreases rather than increases, with Na exposure, argues against Na intercalation. In studies of K on MoS<sub>2</sub> at very low temperatures,<sup>17</sup> the

band gap was seen to increase so that an electronic structure characteristic of the isolated monolayer at the surface of the bulk MoS<sub>2</sub> crystal was noted, as a result of intercalation of K. The effective band gap, of 1.8 eV, as might be inferred from those measurements,<sup>17</sup> places the band gap close to the value predicted by DFT, and the value of 1.9 eV expected based on photoluminescence of monolayer MoS<sub>2</sub>(0001). This minor deviation in the band gap, easily explained by an added Na density of states just below what was formally the MoS<sub>2</sub> monolayer conduction band minimum, argues against a major final state influence on the photoemission spectra due to increased metallicity.

In summary, we obtained the wave vector dependent occupied and unoccupied band structure of the MoS<sub>2</sub>(0001) surface though a combination of angle-resolved photoemission and inverse photoemission. While the exposure of Na to the MoS<sub>2</sub>(0001) surface leads to the expected n-type doping shifts of the bands,<sup>5</sup> this shift in the band binding energies is wave vector independent for the occupied bands, not seen in the case of alkali metal intercalation.<sup>17</sup> From the different shifts seen in photoemission and inverse photoemission we are led to the conclusion that Na exposure increases the metallicity of MoS<sub>2</sub>(0001), consistent with theory.

This work was supported by C-SPIN, part of STARnet, a Semiconductor Research Corporation program sponsored by MARCO and DARPA (SRC 2381.002 and 2381.003). Further, funding was provided through the NSF funded Nebraska MRSEC DMR-0820521 and from DOE grants DE-FG02-07ER15842 (UCR and UCF) and DE-FG02-07ER46354 (UCF). E.F.S. acknowledges financial support by the JSPS postdoctoral fellowship for overseas researchers as well as the Alexander von Humboldt Foundation. The experiments have been performed under the approval of HiSOR (Proposal No. 13-B-36). DFT calculations were performed at the National Energy Research Scientific Computing Center (Project No. 45594).

<sup>1</sup>H. Liu, M. Si, Y. Deng, A. T. Neal, Y. Du, S. Najmaei, and P. M. Ajayan, *ACS Nano* **8**, 1031–1038 (2014).

<sup>2</sup>S. Chuang, C. Battaglia, A. Azcatl, S. McDonnell, J. S. Kang, X. Yin, M. Tosun, R. Kapadia, H. Fang, R. M. Wallace, and A. Javey, *Nano Lett.* **14**, 1337–1342 (2014).

<sup>3</sup>J. R. Chen, P. M. Odenthal, A. G. Swartz, G. C. Floyd, H. Wen, K. Y. Luo, and R. K. Kawakami, *Nano Lett.* **13**, 3106–3110 (2013).

<sup>4</sup>M. S. Choi, G.-H. Lee, Y. J. Yu, D.-Y. Lee, S. H. Lee, P. Kim, J. Hone, and W. J. Yoo, *Nature Commun.* **4**, 1624 (2013).

<sup>5</sup>M. Tosun, S. Chuang, H. Fang, A. B. Sachid, M. Hettick, Y. Lin, Y. Zeng, and A. Javey, *ACS Nano* **8**, 4948–4953 (2014).

<sup>6</sup>L. David, R. Bhandavat, and G. Singh, *ACS Nano* **8**, 1759–1770 (2014).

<sup>7</sup>J. Park, J.-S. Kim, J.-W. Park, T.-H. Nam, K.-W. Kim, J.-H. Ahn, G. Wang, and H.-J. Ahn, *Electrochim. Acta* **92**, 427–432 (2013).

<sup>8</sup>V. P. Santos, B. van der Linden, A. Chojeci, G. Budroni, S. Corthals, H. Shibata, G. R. Meima, F. Kapteijn, M. Makkee, and J. Gascon, *ACS Catal.* **3**, 1634–1637 (2013).

<sup>9</sup>A. Andersen, S. M. Kathmann, M. A. Lilga, K. O. Albrecht, R. T. Hallen, and D. Mei, *J. Phys. Chem. C* **115**, 9025–9040 (2011).

<sup>10</sup>A. Kotarba, G. Adamski, W. Piskorz, Z. Sojka, C. Sayag, and G. Djega-Mariadassou, *J. Phys. Chem. B* **108**, 2885–2892 (2004).

<sup>11</sup>R. Coehoorn, C. Haas, J. Dijkstra, C. J. F. Flipse, R. A. de Groot, and A. Wold, *Phys. Rev. B* **35**, 6195 (1987).

<sup>12</sup>S. K. Mahatha, K. D. Patel, and K. S. R. Menon, *J. Phys.: Condens. Matter* **24**, 475504 (2012).

<sup>13</sup>R. Suzuki, M. Sakano, Y. J. Zhang, R. Akashi, D. Morikawa, A. Harasawa, K. Yaji, K. Kuroda, K. Miyamoto, T. Okuda, K. Ishizaka, R. Arita, and Y. Iwasa, *Nat. Nanotechnol.* **9**, 611–617 (2014).

<sup>14</sup>W. Jin, P.-C. Yeh, N. Zaki, D. Zhang, J. T. Sadowski, A. Al-Mahboob, A. M. van der Zande, D. A. Chenet, J. I. Dadap, I. P. Herman, P. Sutter, J. Hone, and R. M. Osgood, Jr., *Phys. Rev. Lett.* **111**, 106801 (2013).

<sup>15</sup>S. W. Han, G.-B. Cha, E. Frantzeskakis, I. Razado-Colambo, J. Avila, Y. S. Park, D. Kim, J. Hwang, J. S. Kang, S. Ryu, W. S. Yun, S. C. Hong, and M. C. Asensio, *Phys. Rev. B* **86**, 115105 (2012).

<sup>16</sup>T. Komesu, D. Le, Q. Ma, E. F. Schwier, Y. Kojima, M. Zheng, H. Iwasawa, K. Shimada, M. Taniguchi, L. Bartels, T. Rahman, and P. A. Dowben, *J. Phys.: Condens. Matter* **26**, 455501 (2014).

<sup>17</sup>T. Eknapakul, P. D. C. King, M. Asakawa, P. Buaphet, R.-H. He, S.-K. Mo, H. Takagi, K. M. Shen, F. Baumberger, T. Sasagawa, S. Jungthawan, and W. Meevasana, *Nano Lett.* **14**, 1312–1316 (2014).

<sup>18</sup>M. Kamaratos, D. Vlachos, and C. A. Papageorgopoulos, *J. Phys. Condens. Matter* **5**, 535–540 (2014).

<sup>19</sup>C. A. Papageorgopoulos, M. Kamaratos, S. Kennou, and D. Vlachos, *Surf. Sci.* **251**, 1057–1061 (1991).

<sup>20</sup>S. Kennou, S. Ladas, and C. Papageorgopoulos, *Surf. Sci.* **152**, 1213–1221 (1985).

<sup>21</sup>K. T. Park and J. Kong, *Topics in Catalysis* **18**, 175–181 (2002).

<sup>22</sup>K. Shimada, M. Arita, Y. Takeda, H. Fujino, K. Kobayashi, T. Narimura, H. Namatame, and M. Taniguchi, *Surf. Rev. Lett.* **9**, 529 (2002).

<sup>23</sup>T. Komesu, C. Waldfried, H.-K. Jeong, D. P. Pappas, T. Rammer, M. E. Johnston, T. J. Gay, and P. A. Dowben, *Proc. SPIE* **3945**, 6–16 (2000).

<sup>24</sup>P. E. Blöchl, *Phys. Rev. B* **50**, 17953–17979 (1994).

<sup>25</sup>G. Kresse and D. Joubert, *Phys. Rev. B* **59**, 1758–1775 (1999).

<sup>26</sup>G. Kresse and J. Furthmüller, *Phys. Rev. B* **54**, 11169 (1996).

<sup>27</sup>G. Kresse and J. Hafner, *Phys. Rev. B* **47**, 558–561 (1993).

<sup>28</sup>S. Grimme, J. Antony, S. Ehrlich, and H. Krieg, *J. Chem. Phys.* **132**, 154104 (2010).

<sup>29</sup>A. M. Scheer and P. D. Burrow, *J. Phys. Chem. B* **110**, 17751 (2006).

<sup>30</sup>P. D. Burrow and A. Modelli, *SAR QSAR Environ. Res.* **24**, 647–659 (2013).

<sup>31</sup>*Gmelin Handbook of Inorganic and Organometallic Chemistry* (Springer-Verlag, Berlin, 1995).

<sup>32</sup>M. Kamaratos, V. Saltas, C. A. Papageorgopoulos, W. Jaegermann, C. Pettenkofer, and D. Toni, *Surf. Sci.* **402–404**, 37 (1998).

<sup>33</sup>See supplementary material at <http://dx.doi.org/10.1063/1.4903824> for the Na deep 1s and shallow 2p core level spectra.

<sup>34</sup>B. Xu, J. Choi, A. N. Caruso, and P. A. Dowben, *Appl. Phys. Lett.* **80**, 4342–4344 (2002).

<sup>35</sup>P. A. Dowben, J. Xiao, B. Xu, A. Sokolov, and B. Doudin, *Appl. Surf. Sci.* **254**, 4238–4244 (2008).

<sup>36</sup>J. E. Ortega, F. J. Himpsel, D. Li, and P. A. Dowben, *Solid State Commun.* **91**, 807–811 (1994).

<sup>37</sup>J. Xiao and P. A. Dowben, *J. Mater. Chem.* **19**, 2172–2178 (2009).

<sup>38</sup>M. Boehme, R. Adelung, L. Kipp, and M. Skibowski, *Appl. Surface Science* **123–124**, 91–94 (1998).